Journal of Engineering Managment and Soft Computing (JEMSC)

A Robust and Practical Adaptive Inverse Control Scheme for Vehicle Path Tracking: Analysis and Comparative Evaluation

Alireza Borjali[1], Reza Ghasemi[2]✉ and Muhammad Amin Rezaei [3]

1. Department of Electrical Engineering, University of Qom, Qom, Iran. Email: Aborjali1370@gmail.com
2 .Corresponding Author Department of Electrical Engineering, University of Qom, Qom, Iran. Email: r.ghasemi@qom.ac.ir
3. Department of Electrical Engineering, University of Qom, Qom, Iran. Email: Marezaei1380@gmail.com

Article Info

Article type:
Research Article

Article history:
Received: 8 December 2025
Revised: 2 February 2026
Accepted: 8 March 2026
Published online 1 April 2026

Keywords:
Inverse neural network, adaptive inverse control, path planning, back-ropagation algorithm, neural network, model-free controller, multilayer perceptron.

ABSTRACT

This paper addresses an adaptive inverse dynamic control (AIDC) to designate a robust controller for the nonlinear model of the vehicle systems. Compared to prior research that focuses on the intelligent identification of nonlinear systems, the deliberated methodology evolved the inverse intelligent process as a universal controller for a class of nonlinear systems, and this method has achieved a remarkably low root mean square (RMS) and tracking error rate. In the vehicle systems, the tracking of the predefined desired path is challenging to achieve, especially in the presence of disturbances. The planned AIDS procedure consists of an online inverse model identifier updated using the back-propagation (BP) algorithm. In this approach, an offline identification phase provides the initial network weights. A Multilayer Perceptron (MLP) is then employed as a nonlinear controller, trained to represent the system's inverse dynamics and applied to the vehicle model. The convergence of the noisy states to the nominal ones, the robustness of the recommended designing system, and the reduction of noisy phenomena effect in the system's state are all crucial advantages of the planned AIDC. Simulation results demonstrate the promising performance of the proposed methodology.

Cite this article: Ghasemi, R. & et al, (2026)., A Robust and Practical Adaptive Inverse Control Scheme for Vehicle Path Tracking: Analysis and Comparative Evaluation. *Engineering Management and Soft Computing,* 12 (2). 225-241.

DOI: https://doi.org/10.22091/jemsc.2026.14801.1331

Publisher: University of Qom
DOI: https://doi.org/10.22091/jemsc.2026.14801.1331

HIGHLIGHT:

- Proposes a novel two-stage Adaptive Inverse Control (AIC) framework for robust path tracking in vehicle systems with nonlinear, non-affine dynamics.
- Develops a neuro-based methodology where a Multilayer Perceptron (MLP) directly identifies the system's inverse dynamics as a model-free controller.
- Introduces a hybrid learning strategy, combining offline Levenberg-Marquardt initialization with online Backpropagation adaptation for real-time disturbance rejection.
- Enhances inverse neuro-dynamic methodologies by solving the vehicle handling inverse dynamics problem without requiring an explicit analytical model.
- The proposed method solves the vehicle handling inverse dynamics problem.
- Demonstrates precise control performance through simulation, with tracking error converging to near-zero under disturbed conditions.

1) Introduction

As the automobile industry advances rapidly, the surge in vehicle numbers has led to increasingly congested roads, resulting in a significant rise in traffic accidents. Globally, traffic accidents claim approximately 1.3 million lives and injure over 20 million people annually (Abay et al., 2013), and The U.S. Department of Transportation's National Highway Traffic Safety Administration released its early estimates of traffic fatalities for 2024, projecting that 39,345 individuals died in traffic crashes (NHTSA, 2025). Moreover, 93% of motor vehicle accidents are attributed to human error, indicating that drivers often struggle to execute collision avoidance (Maddox, 2012). Consequently, developing effective solutions for emergency collision avoidance has become a critical research focus in the automotive field.

These accidents primarily stem from two key factors: first, the driver's misjudgment of vehicle travel risks, and second, operational errors or delayed reactions. Due to these human limitations, collision avoidance technology for autonomous vehicles has emerged as a critical research priority in the field of intelligent transportation systems (He et al., 2018). An Active Collision Avoidance System (ACAS) is an intelligent vehicular safety system that autonomously detects imminent collision risks using sensors (e.g., radar, LiDAR, cameras) and executes corrective actions, such as braking, steering, or throttle control, to prevent or mitigate accidents. Path tracking control has emerged as a critical component of ACAS. In particular, path planning in emergency avoidance has become an active area of investigation, with numerous studies contributing to advancements in this field (Zhao et al., 2021).

The conceptual framework of this study is grounded in the pioneering work on Adaptive Inverse Control (AIC) established by Widrow and Walach (2008). Their core architecture, which employs an adaptive inverse model of the plant as the controller, provides the foundational abstraction for the control strategy developed herein. This study focuses on the application and rigorous evaluation of this paradigm to the specific and challenging problem of high-speed autonomous vehicle path tracking, where robustness to disturbances and real-time computational efficiency are paramount. In the domain of integrated vehicle control, the seminal work of Falcone et al. (2007), which applied Model Predictive Control (MPC) to combined active steering and braking, established a benchmark for performance and constraint handling in path tracking. Their approach, explicitly formulated to handle tire nonlinearities and maintain stability on slippery surfaces through slip angle constraints, demonstrated that MPC could reliably execute complex maneuvers such as the double lane change. The application of neural networks to autonomous vehicle control has notable historical precedents. The foundational use of neural networks for autonomous vehicle guidance was demonstrated by Pomerleau's ALVINN (Autonomous Land Vehicle in a Neural Network) project (Pomerleau, 1989). This early system employed a three-layer backpropagation network to perform road-following by directly mapping visual sensor inputs to steering commands, establishing a critical proof of concept for data-driven vehicle control. Its success

illustrated the potential of multilayer perceptrons to learn complex control policies from sensory data, a principle that informs the neural architectures used in contemporary research.

Shim et al. (2012) presents an autonomous vehicle collision avoidance system that integrates path planning with MPC to coordinate active front steering and wheel torque control. Salepour et al. (2015) introduces an integrated controller based on Linear Quadratic Regulator (LQR) that establishes an optimized tracking function and controls the yaw moment. Kim et al. (2012) presents an infrastructure-based path-tracking control system designed to guide vehicles safely from a start point to a destination while avoiding obstacles. A key advantage of using MPC for collision avoidance is its ability to constantly optimize performance by updating real-time data on the vehicle's position, heading angle, and surrounding obstacles. Hassanzadeh et al. (2012) employs a polynomial trajectory to determine feed-forward control inputs and implemented a feedback controller utilizing a proportional-derivative (PD) approach to correct yaw angle errors resulting from nonlinearity and uncertainty in autonomous collision avoidance systems. Cao et al. (2017) proposes a controller architecture for emergency lateral collision avoidance through integrated automatic steering and braking control. Feedforward control ensures precise path following, while feedback control stabilizes the vehicle and minimizes tracking errors. An enhanced reinforcement learning algorithm was implemented to develop an obstacle avoidance control framework, enabling autonomous vehicles to perform continuous action maneuvers (Zong et al., 2017). The study conducted by Ji et al. (2017) proposes an integrated path planning and tracking framework designed to ensure collision-free navigation for autonomous vehicles. Therefore, this introduces a multi-constrained model predictive control approach for trajectory tracking, incorporating full vehicle dynamics. Extensive simulations under varying conditions demonstrate the controller's effectiveness. Wang et al. (2017) proposed a collision avoidance system that integrates a path planner with a robust tracking controller. Guo et al. (2016) presents a dynamic control framework for vision-based autonomous vehicles, focusing on coordinated steering and braking control during emergency obstacle avoidance. First, a real-time vision algorithm is developed to detect the reference path and estimate the vehicle's local position relative to the path. Subsequently, a novel coordinated control strategy is proposed, combining nonlinear backstepping control theory with adaptive fuzzy sliding-mode control to ensure robust performance. The asymptotic stability of the closed-loop system is rigorously proven using Lyapunov theory. He et al. (2018) introduces a hierarchical emergency steering control strategy designed to avoid collision while maintaining vehicle stability under dynamic driving conditions near handling limits. The proposed architecture comprises a high-level decision-making module and a low-level motion controller. Zhao et al. (2021) proposes an Adaptive Inverse Control (AIC) approach to address vehicle handling inverse dynamics for emergency path tracking control. The proposed AIC system comprises two neural network-based adaptive filter modules: (1) a model identifier that captures the vehicle's nonlinear characteristics, and (2) an inverse model controller that solves the dynamics inversion problem. Then, the backpropagation algorithm dynamically adapts the model identifier's weight parameters to enable real-time identification of the vehicle's nonlinear dynamic characteristics. Simultaneously, the inverse model controller serves as the AIC system's primary control module, with its weight parameters continuously adjusted online via the backpropagation-through-model (BPTM) algorithm. Shah et al. (2015) presents a hierarchical rear-end collision avoidance system for autonomous vehicles, consisting of linear threat assessment module, an escape path planner accommodating non-zero initial conditions, a reference path generator, and a linear state feedback controller.

Given that vehicle dynamics represent time-varying systems subject to external disturbances, robust control methods have been incorporated into the path following framework to ensure disturbance rejection. The path following control architecture combines backstepping methodology with two disturbance-rejection strategies: adaptive fuzzy sliding mode control for parameter variations and neurodynamic optimization for external disturbances (Peng et al., 2019). Dong et al. (2024) proposed an integrated MPC framework for the simultaneous path planning and tracking control of autonomous vehicles in dynamic environments. The method formulates collision avoidance as a constrained optimization problem, using a vehicle kinematic model to predict future states over a finite horizon. Wang et al. (2016) presents an H_∞-based robust control strategy for autonomous vehicle path following

under challenging operational conditions, including time delays, intermittent data losses, parameter uncertainties, and external disturbances. The controller design incorporates a generalized delay model while explicitly accounting for tire cornering stiffness variations, with the H_∞ framework providing guaranteed performance bounds. Chen et al. (2023) introduces a disturbance-adaptive control method for vehicle stability under varying road conditions. Liu et al. (2020) introduces a feed-forward controller designed for four-wheel steering autonomous vehicles to accurately track the desired yaw rate. Additionally, to address tracking errors arising from vehicle nonlinearity and external disturbances, an active disturbance rejection control (ADRC) feedback controller is developed to precisely follow the desired lateral displacement and yaw angle. All proposed emergency avoidance controllers demonstrate satisfactory performance within their respective operational envelopes, validating their effectiveness under specific working conditions.

The essence of path tracking control lies in determining the vehicle's steering wheel angle. The most effective approach for path planning is to address the inverse dynamics problem. This approach can effectively generate appropriate inputs to achieve the desired output. While robust feedback controllers (e.g., MPC, LQR) excel in disturbance rejection, their computational complexity and reliance on accurate, real-time state measurement can be limiting for high-frequency control tasks or resource-constrained platforms. Inverse control, particularly in its adaptive form, offers a fundamentally different paradigm: it learns a direct mapping from desired output to required input. When initialized with a robust offline model and endowed with a stability-guaranteed online adaptive element, this approach can achieve disturbance rejection through not only error feedback, but also predictive model correction. This work explores this alternative paradigm, arguing that it can provide a highly efficient and robust solution, particularly when computational resources are at a premium. As an open-loop approach, inverse neural network control avoids the instability issues associated with feedback. In Quintero-Manriquez et al.'s (2019) study, a discrete-time neural inverse optimal controller was developed for induction motors. A recurrent high-order neural network (RHONN) serves as the model identifier, with training performed using the extended Kalman filter (EKF). Simulation results demonstrate the controller's robustness against parameter variations and external disturbances.

In this paper, we propose a novel two-stage hybrid AIDC framework to solve the vehicle handling inverse dynamics problem for precise path tracking and emergency collision avoidance. The core methodological novelty lies in employing a Multilayer Perceptron (MLP) to directly identify and act as the system's inverse model—a model-free, nonlinear controller. The architecture uniquely integrates offline Levenberg-Marquardt training for stable initialization with online Backpropagation (BP) for real-time adaptive adjustment, creating a robust controller resilient to disturbances. This methodology effectively constitutes an adaptive open-loop control strategy, inherently avoiding feedback-induced instability while minimizing overshoot, rise time, and steady-state error. Crucially, the proposed AIDC does not require the dynamical model of the process. Comprehensive simulation studies demonstrate the framework's efficacy in ensuring robustness and driving the tracking error to converge to near zero, showcasing its potential as a computationally efficient and robust alternative to existing control paradigms. While deep reinforcement learning (DRL) and model predictive control (MPC) dominate recent literature, their need for extensive tuning, computational resources, or accurate models can be prohibitive. Therefore, this paper comprehensively demonstrates that a well-designed AIDC, leveraging modern computational tools, remains a highly competitive, simple, and robust solution for path tracking, particularly under significant sensor noise and disturbances.

The remainder of the paper is structured as follows: the second section presents the nonlinear vehicle dynamic model, while the third section discusses the design and modeling of the adaptive MLP inverse controller. The fourth section examines the simulation results, and the final section concludes the paper.

2) Nonlinear Dynamical Model of Vehicle

In this study, a 2-DOF bicycle tracking model is employed for the design of the controller. To train the neural network, a vehicle dynamics model must be developed to generate data on vehicle dynamics

characteristics, which is free from disturbances and noise. Assuming a constant longitudinal velocity, two degrees of freedom (2-DoF) vehicle dynamics model, incorporating lateral velocity v and yaw rate ω, is developed based on the assumptions presented in Hu et al. (2016), as illustrated in Figure 1.

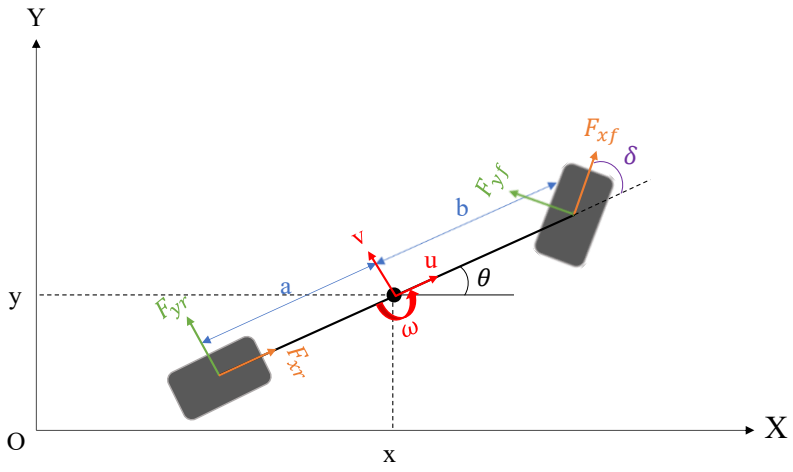

Figure 1. 2-DoF Vehicle Dynamics Model

Based on Newton's laws, the differential equations of vehicle motion are derived and can be formulated as follows (Zhao et al., 2021):

$$\begin{cases} m(\dot{v} + u\omega) = 2F_{yf}\cos\delta + 2F_{yr} \\ I_z\dot{\omega} = 2aF_{yf}\cos\delta - 2bF_{yr} \end{cases} \quad (1)$$

where m denotes the total mass of the vehicle, I_z represents the rotational inertia about the vertical axis, v and u correspond to the lateral and longitudinal velocities of the vehicle, a and b denote the distances from the center of mass to the front and rear axles, F_y represents the lateral force of the wheel. f denotes the front wheel, and r denotes the rear wheel.

The lateral tire forces F_y can be calculated using the "Magic Formula" tire model (Bakker et al., 1987), expressed as follows:

$$F_y = D\ \ sin(\ C\ tan^{-1}(B\Phi)) + S_v \quad (2)$$

The parameters B, C, D, and S_v represent the stiffness factor, shape factor, peak factor, and vertical shift, respectively. Subsequently, Φ can be denoted by (Zhao et al., 2021):

$$\Phi = (1 - E)(\alpha - S_h) + (\frac{E}{B})\ tan^{-1}(B(\alpha + S_h)) \quad (3)$$

where α refers to the slip angle of wheel, E refers to the curvature factor, S_h refers to the horizontal shift. Slip angle can be described as

$$\begin{cases} \alpha_f = \delta - tan^{-1}(\dfrac{v + a\omega}{u}) \\ \alpha_r = -tan^{-1}(\dfrac{v - b\omega}{u}) \end{cases} \quad (4)$$

In addition, peak factor (D) and curvature factor (E) can be expressed by vertical load F_z as:

$$\begin{cases} D = a_1F_z^2 + a_2F_z \\ (BCD) = a_3\ sin(a_4\ \ tan^{-1}(a_5F_z)) \\ B = (BCD)/C\ D \\ E = a_6F_z^2 + a_7F_z + a_8 \end{cases} \quad (5)$$

According to the loss of complexity and simplification, S_v, S_h are equal to zero and the camber angle of wheel, the lateral and longitudinal loads transfer during vehicle driving are overlooked. Additionally, the shape factor is equal to C = 1.3. The vertical loads on wheel can be subsequently calculated by

$$\begin{cases} F_{z1} = \dfrac{1}{2}\dfrac{mgb}{a+b} \\ F_{z2} = \dfrac{1}{2}\dfrac{mga}{a+b} \end{cases} \tag{6}$$

where g is the acceleration of gravity.

The front wheel angle δ is determined by the steering wheel angle δ_{sw} and the steering system's angle transmission ratio i_{sw} as

$$\delta = \frac{\delta_{sw}}{i_{sw}} \tag{7}$$

However, a rigid vehicle model is optimal for practical occasions, while complexity is relevant to the number of degrees of freedom. According to the structure of front-wheel steering vehicle, a four-wheel vehicle can be modeled as a simple bicycle. Assuming kinematic model, the slip between wheel and road can be ignored. Therefore, the kinematic model of vehicle can be expressed as

$$\begin{cases} \dot{x} = u\cos\theta \\ \dot{y} = u\sin\theta \end{cases} \tag{8}$$

The relationship between the yaw rate ω and the yaw angle θ can be expressed as follows:

$$\dot{\theta} = \omega \tag{9}$$

3) Adaptive Inverse MLP Controller

3-1) The Structure of controller System

The primary concept of AIC is to utilize an inverse model of the plant as a controller to drive the system's output toward a specified reference. By incorporating an inverse model, AIC ensures that the plant's output closely tracks the desired trajectory, even in the presence of disturbances or nonlinearities.

To achieve high tracking accuracy, a neural network is employed as the inverse model identifier. The neural network is trained using a Backpropagation (BP) algorithm, which optimizes the model parameters to minimize the error between the plant's output and the reference. The inverse model is serialized with the main system, effectively creating an identity function that ensures the output faithfully follows the input reference.

The inverse model identifier (IMI) utilizes the inputs and outputs of the primary plant, along with their delayed forms, as its inputs. To enhance robustness against faults and external disturbances, an adaptive BP algorithm has been developed for the IMI, enabling online adjustment of the neural network weights, as illustrated in Figure 2. These optimized weights are subsequently applied to the inverse model controller to ensure effective control performance.

Consequently, the AIC system ensures precise tracking of the desired reference trajectory, even in the presence of faults and external disturbances.

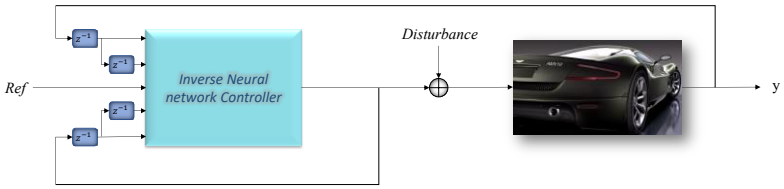

Figure 2. The AIDC System for Vehicle

3-2) Online Modeling Using MLP

The neural networks as a universal approximators have high accuracy in modeling of the nonlinear complex systems. In this study, the MLP algorithm has been employed to estimate the proposed system.

3-2-1) MLP Algorithm Structure

The architecture of the MLP neural network, presented in Figure 3, consists of one input layer, one hidden layer, and one output layer. The input vector, hidden layer neuron vector, and output vector are denoted as U, O, and Y, respectively, and are defined as follows:

$$\begin{cases} U = [u_1\ u_2\ \cdots\ u_i\ \cdots\ u_n]^T, i = 1,2,\cdots,n \\ O = [o_1\ o_2\ \cdots\ o_j\ \cdots\ o_m]^T, j = 1,2,\cdots,m \\ Y = [y] \end{cases} \tag{10}$$

Here, n represents the number of nodes in the input layer, and m denotes the number of nodes in the hidden layer. Each u_i corresponds to the ith input, while o_j represents the jth neuron in the hidden layer. the number of hidden layer neurons is ten. Thus, n = 5 and m = 10.

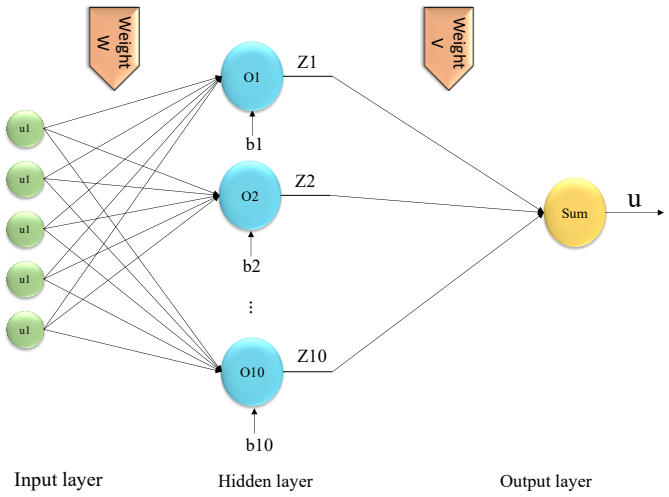

Figure 3. The Structure of MLP Neural Network

The hidden layer employs a nonlinear activation function, denoted as g, while the output layer utilizes a linear activation function, denoted as f. The activation functions are written as:

$$\begin{cases} g(x) = \dfrac{1}{1+e^{-x}} \\ \dfrac{\partial g(x)}{\partial x} = (\dfrac{1}{1+e^{-x}})(1-\dfrac{1}{1+e^{-x}}) \\ f(x) = x \\ \dfrac{\partial f(x)}{\partial x} = 1 \end{cases} \tag{11}$$

The nonlinear difference equation, denoted as D(.), which relates the output longitudinal distance y to the input yaw angle u, can be expressed as follows:

$$y(k) = D(u(k), u(k-1), u(k-2), y(k-1), y(k-2)) \tag{12}$$

Therefore, the inverse of equation (8) can be calculated as

$$u(k) = D^{-1}(u(k-1), u(k-2), y(k), y(k-1), y(k-2)) \tag{13}$$

Using the above difference model, the neural networks, presented in Figure 4, as both the model identifier and the inverse model identifier involve five inputs, ten neurons, and one output.

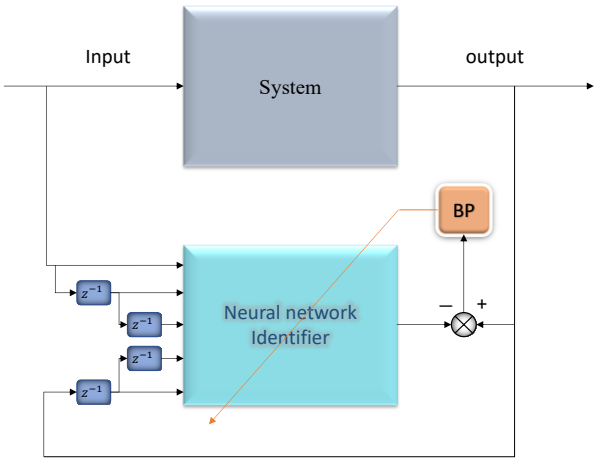

(a)

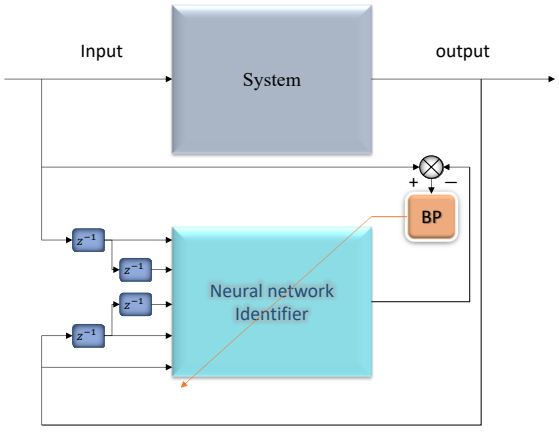

(b)

Figure 4. The Block Diagram of Training Using BP Neural Network: Model Identifier (a), and Inverse Model Identifier (b)

3-2-1) Adaptive Algorithm for Online Learning in MLP

Due to the equation (10) and the structure of MLP for desired system, the output of inverse MLP neural network can be denoted by:

$$u_{hat} = V^T \times Z \tag{14}$$

Where V is the weight with dimensions of 10×1, and Z, as outputs of the hidden layer, can be expressed as:

$$Z_{j1} = g(S_{j1}) \qquad ,j = 1,2,\cdots,10 \tag{15}$$

S, as the inputs of the hidden layer, can be shown as follows:

$$S_{j1} = (W^T \times U) + B_j \qquad ,j = 1,2,\cdots,10 \tag{16}$$

where the dimension of input weights W is 5×10, the bias B is 10×1, and U represents the input of MLP neural network.

The gradient descent method and the BP algorithm are applied to update the nonlinear parameters B, W, and V online. The error function I can be expressed as follows:

$$I^q = \|u^q - {u_{hat}}^q\|^2 \, , q = 1,2,\cdots,Q \tag{17}$$

Where Q is the number of observations. Consequently, the gradient descent is written as:

$$\begin{cases} w_{ij}^{new} = w_{ij}^{old} - \rho \dfrac{\partial I^q}{\partial w_{ij}^{old}} \\ i = 1,2,\cdots,5 \qquad j = 1,2,\cdots,10 \end{cases} \tag{18}$$

where ρ is the learning rate of network.

According to equation (18), the derivative of the error function respect to the W should be calculated in equation (19).

$$\frac{\partial I^q}{\partial w_{ij}} = \frac{\partial}{\partial w_{ij}} \|u^q - {u_{hat}}^q\|^2 = -2(u^q - {u_{hat}}^q) \frac{\partial u_{hat}}{\partial w_{ij}} \tag{19}$$

The derivative of the MLP output respect to the W can be expressed by:

$$\frac{\partial u_{hat}}{\partial w_{i\,j}} = \frac{\partial}{\partial w_{i\,j}} (\sum_{k=1}^{m} Z_k \, v_{k1}) = v_{k1} \frac{\partial Z_k}{\partial w_{i\,j}} \tag{20}$$

Therefore, the derivative of the output neuron respect to the W can be expressed as:

$$\frac{\partial Z_m}{\partial w_{i\,j}} = \frac{\partial g(S_m)}{\partial w_{i\,j}} \, , m = 1,2,\cdots,10 \tag{21}$$

Now, the chain rule can support to calculate the above derivative.

$$\frac{\partial g(S_m)}{\partial w_{i\,j}} = \frac{\partial g(S_m)}{\partial S_m} \times \frac{\partial S_m}{\partial w_{i\,j}} = \frac{\partial g(S_m)}{\partial S_m} U_m \tag{22}$$

Using equations (20), (21), and (22), the equation (23) can be rewritten as:

$$\frac{\partial I^q}{\partial w_{ij}} = -2(u^q - {u_{hat}}^q) v_{k1} U_k \frac{\partial g(S_k)}{\partial S_k} \tag{23}$$

Due to equation (23), the equation (18) can be reconstructed as:

$$w_{ij}^{new} = w_{ij}^{old} + \rho 2(u^q - {u_{hat}}^q) v_{k1} U_k \frac{\partial g(S_k)}{\partial S_k} \tag{24}$$

In next step, V parameters can be adjusted using the gradient descent method.

The error function I is proposed by:

$$I^q = \|u^q - {u_{hat}}^q\|^2 , q = 1,2,\cdots,Q \tag{25}$$

Using the gradient descent, the update rules are shown as:

$$\begin{cases} v_{ij}^{new} = v_{ij}^{old} - \rho \dfrac{\partial I^q}{\partial v_{ij}^{old}} \\ i = 1,2,\cdots,5 \qquad j = 1,2,\cdots,10 \end{cases} \tag{26}$$

The derivative of the error function respect to the V weight can be reestablished as follows:

$$\frac{\partial I^q}{\partial v_{i1}} = \frac{\partial}{\partial v_{i1}} \|u^q - {u_{hat}}^q\|^2 = -2(u^q - {u_{hat}}^q) \frac{\partial u_{hat}}{\partial v_{i1}} \tag{27}$$

$\frac{\partial u_{hat}}{\partial v_{i1}}$ can be determined as follows:

$$\begin{cases} \dfrac{\partial u_{hat}}{\partial v_{i\,1}} = \dfrac{\partial}{\partial v_{i\,1}} \left(\sum_{k=1}^{m} Z_{k1}\, v_{k1}\right) = Z_m \\ m = 1,2,\cdots,10 \end{cases} \tag{28}$$

By equations (27) and (28), the update rules of V are:

$$v_{ij}^{new} = v_{ij}^{old} + \rho 2(u^q - {u_{hat}}^q) Z_m \tag{29}$$

Similarly, the bias can be optimized based on equations (19), (20), and (21) as follow:

$$\begin{cases} b_j^{new} = b_j^{old} - \rho \dfrac{\partial I^q}{\partial b_j^{old}} \\ b_j^{new} = b_j^{old} + \rho 2(u^q - {u_{hat}}^q) v_{k1} \dfrac{\partial g(S_k)}{\partial S_k} \\ j = 1,2,\cdots,10 \quad , \quad k = 1,2,\cdots,10 \end{cases} \tag{30}$$

MLP Algorithm: The procedures of MLP system design are presented as follows:

Step 1: offline inverse model identification

Construct the MLP neural network structure with the Levenberg–Marquardt algorithm, which can be expressed by equation (14).

Step 2: adjust weighting parameters online using the BP algorithm

Use error function, which is represented in equation (17), and substitute it into gradient descent equation (18).

According to equations (17) and (18), weight and bias adjustment equations (24), (29), and (30) can be obtained.

Step 3: Copy the new weights and bias into the controller

Inverse model controller structure is similar to inverse model identifier structure.

Step 4: Go to step 2

4) Simulation Results

All the proposed methods presented in last sections are applied to the nonlinear model of vehicle. Vehicles must perform collision avoidance maneuvers to navigate around other vehicles or obstacles when traveling at high speeds. In this case, As depicted in Figure 5, the schematic diagram of the emergency avoidance maneuver specifies the lane change width as 3m, and the longitudinal distance as 240 m. The vehicle parameters are presented in Table 1.

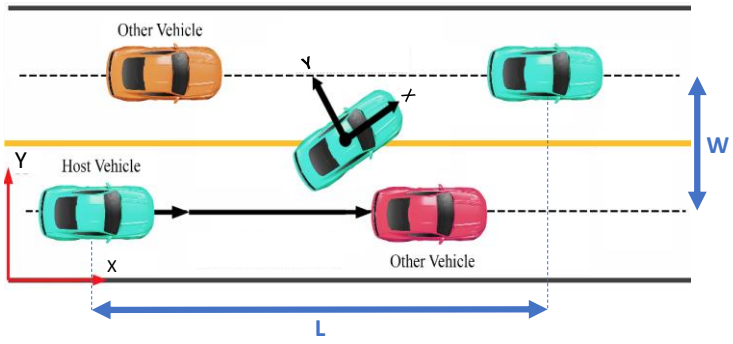

(a)

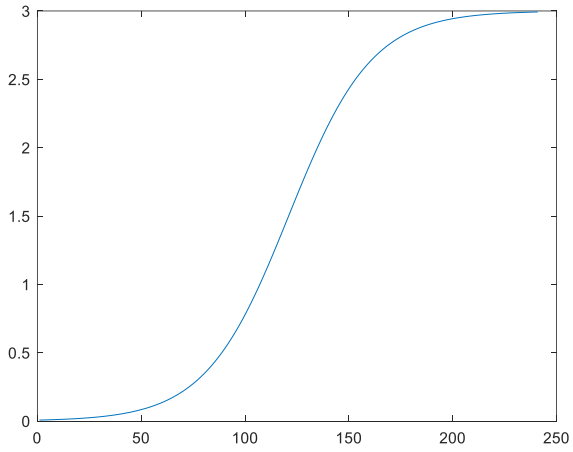

(b)

Figure 5. Collision Avoidance Maneuver (a), and Desired Collision Avoidance Path (b)

Table 1. Vehicle Parameters

symbol	value	symbol	value
z	1416 kg	I_z	1523 $kg.m^2$
a	1.016 m	b	1.526 m
u	20 m/s	i_{sw}	29.5
a1	-22.1	a2	1011
a3	1078	a4	1.82
a5	0.208	a6	0
a7	-0.354	a8	0.707

Case 1: Simulation Results of Offline Phase

The neural network was employed to model and identify the inverse system kinematics, leveraging its capability to approximate complex nonlinear relationships. The training process was conducted using MATLAB's Neural Network Toolbox, with the network architecture and training parameters optimized to achieve high accuracy. The training process utilized the Levenberg-Marquardt algorithm, a robust method for minimizing the mean squared error (MSE) performance metric. The data division was randomized to ensure unbiased training, validation, and testing subsets. Key training parameters and results are summarized as follows:

Epochs: The training concluded after reaching the maximum number of epochs (1000), with the final performance metric (MSE) converging to 6.24×10^{-6}, indicating a high level of accuracy.

Gradient: The gradient magnitude decreased from 4.88 to 0.000804, suggesting that the optimization process approached a local minimum.

Mu (Regularization Parameter): The parameter stabilized at 1×10^{-9}, reflecting a balance between the Gauss-Newton and gradient descent methods during training.

Validation Checks: Only 1 validation check was triggered out of a maximum of 6, confirming the effective mitigation of overfitting.

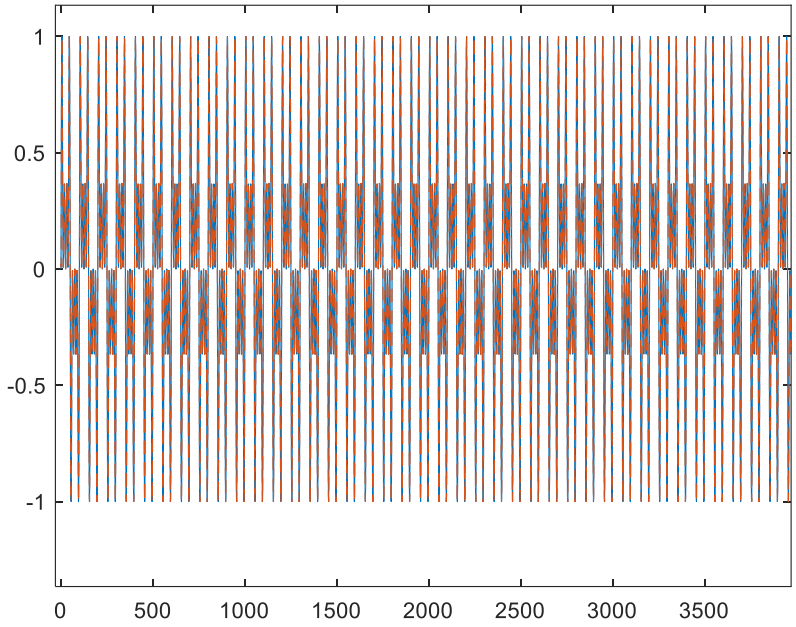

Figure 6. Offline Inverse Kinematics Tracking

Case 2: Simulation Results of MLP Network

The proposed model and inverse model identifier based on MLP neural network are discussed in here. In this simulation scenario, a total of 240 training epochs was implemented, corresponding to a road distance, while the learning rate is chosen 0.27. The fault in input of the system is considered additive with a range of $\pm 5\%$.

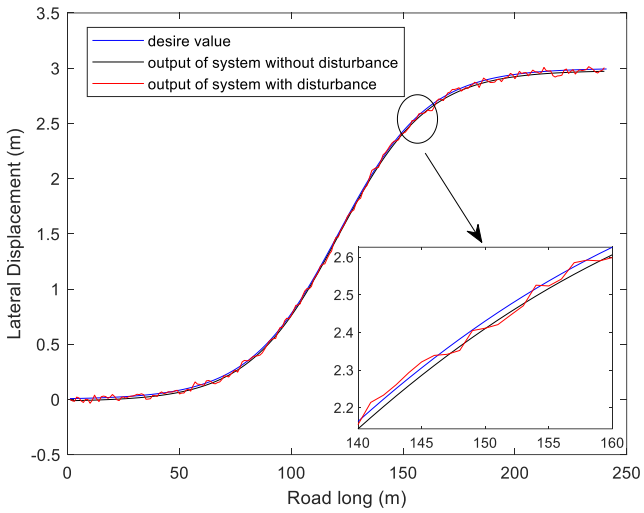

(a)

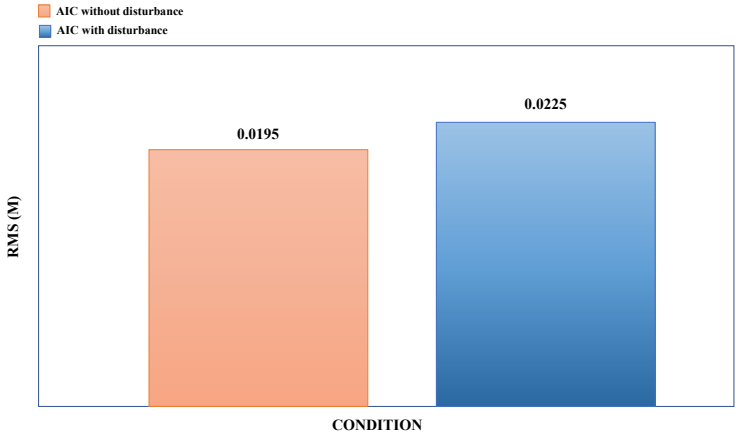

(b)

Figure 7. The Simulation Results for Tracking the Desired Path with MLP Neural Network (a), and the Root Mean Square (RMS) of Error (b)

The robustness of the control method is demonstrated in Figure 7, where trajectory tracking performance is shown with and without external disturbances. To prove the performance of controllers, the root mean square (RMS) of the lateral displacement error is computed and presented in Figure 7, part b. As shown in Figure 7, AIDC, with the MLP neural network, can damp the effects of disturbance on the system output. Figure 8 illustrates the control signal and the effect of the faults on the control input to fix the faults.

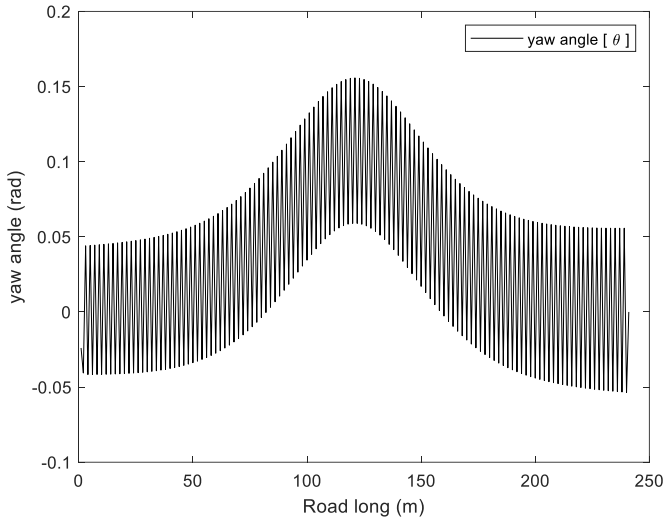

Figure 8. The Control Signal of AIDC with MLP Neural Network

The error between desired output and AIDC output can be shown in Figure 9.

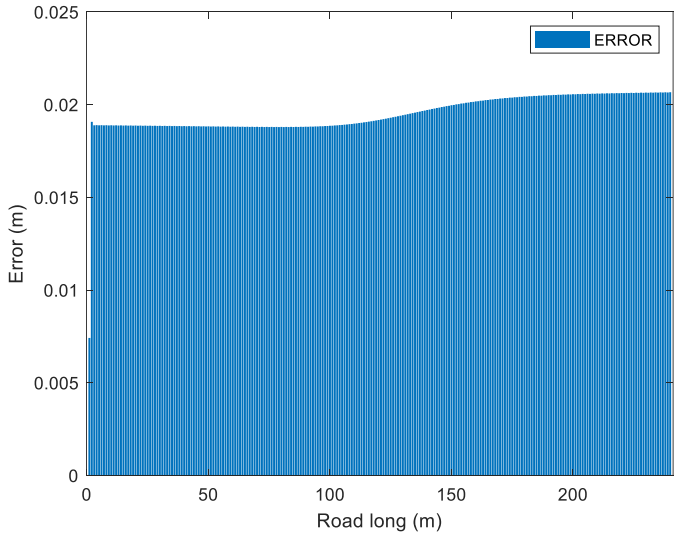

Figure 9. The Error of AIDC with MLP Neural Network

The accuracy of performance or error between the AIDC output and the desired output in this method follows the order of 10^{-4}, which is considered an acceptable accuracy. The maximum error and the RMS of control system without disturbances are 0.0207m and 0.0195m, respectively. When the disturbances are applied, the peak of error for the AIC method rises to 0.0571m, while the RMS increases to 0.0225m. The experimental results confirm the AIC system's disturbance rejection capability, enabling precise trajectory tracking even in noisy environments. This robustness makes it particularly suitable for vehicle emergency avoidance scenarios.

4-1) Path Tracking Performance Analysis: SARSA Reinforcement Learning Controller

This comparative analysis evaluates the performance of the proposed path tracking controller against a SARSA (State-Action-Reward-State-Action) reinforcement learning implementation. The RL controller utilizes a discretized Q-learning approach with a three-dimensional state space comprising lateral error,

longitudinal error, and yaw rate. The system employs an adaptive learning rate ($\alpha = 0.3 \rightarrow 0.01$), ε-greedy exploration ($\varepsilon = 0.5 \rightarrow 0.05$), and a reward function, balancing tracking accuracy against control effort. Vehicle dynamics are modeled using a simplified bicycle model with 20 m/s constant velocity.

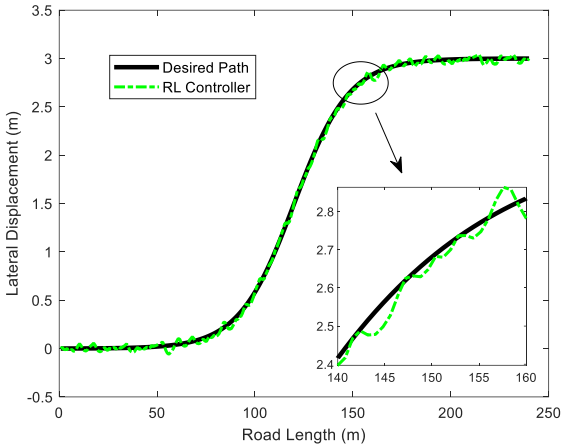

(a)

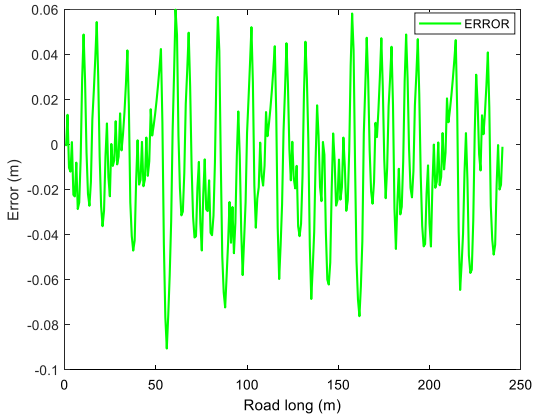

(b)

Figure 10. The Simulation Results for Tracking the Desired Path with SARSA RL(A), and the Error of SARSA RL (b)

4-2) Comparative Analysis with SARSA Reinforcement Learning RL

The proposed controller demonstrates superior tracking precision with an RMS error of 0.0225 m, compared to the RL controller's RMS error of 0.0312 m. This represents a 27.9% reduction in tracking error, indicating that the proposed method achieves approximately 28% better accuracy in following the collision avoidance path. The lower RMS value signifies consistently smaller deviations from the desired trajectory throughout the 240-meter path, resulting in smoother and more precise vehicle control. Peak error analysis reveals the proposed controller's maximum deviation of 0.0571 m, compared to the RL controller's 0.061 m peak error, representing a 6.4% improvement in worst-case scenario performance. While both controllers maintain sub-10-centimeter error bounds, the proposed method demonstrates slightly better containment of extreme tracking deviations, indicating enhanced robustness against challenging path segments. While the RL controller shows competitive performance with its adaptive learning capabilities, the proposed controller's algorithmic design appears to offer more consistent error minimization across varying path curvatures and regions. This performance gap

suggests that the proposed method may better handle the dynamic challenges presented by the changing curvature of collision avoidance path, particularly in the steeper middle section where tracking demands are the highest.

5) CONCLUSION

This paper has presented an applicable two-stage Adaptive Inverse Control (AIC) framework for robust vehicle path tracking. The core methodological contribution is the use of a Multilayer Perceptron (MLP) to directly identify the system's inverse dynamics as a model-free controller, uniquely combining offline initialization using the Levenberg-Marquardt algorithm by online adaptation via Backpropagation (BP). This hybrid structure enables real-time robustness to disturbances without relying on an explicit analytical model of the vehicle. Comprehensive simulation studies confirm the efficacy of the framework: it successfully generates precise control inputs for accurate path following, with both peak error and RMS values maintained within stringent thresholds under disturbed conditions. Future research will focus on the experimental validation of this AIC strategy, implementing it on a scaled vehicle testbed or hardware-in-the-loop (HIL) platform to bridge the gap between simulation and real-world deployment. Further exploration will also investigate integrating deep learning architectures to enhance feature extraction and adaptability in more complex environments.

References

Abay, K. A., Paleti, R., & Bhat, C. R. (2013). The joint analysis of injury severity of drivers in two-vehicle crashes accommodating seat belt use endogeneity. *Trans. Res. B-Meth, 50*, 74-89.

Abay, K. A., Paleti, R., & Bhat, C. R. (2013). The joint analysis of injury severity of drivers in two-vehicle crashes accommodating seat belt use endogeneity. *Transportation research part B: methodological*, *50*, 74-89. https://doi.org/10.1016/j.trb.2013.01.007

NHTSA (2025, April). https://www.nhtsa.gov/press-releases/nhtsa-estimates-39345-traffic-fatalities-2024

Maddox, J. (2012). Improving driving safety through automation. National Highway Traffic Safety Administration.

Maddox, J. (2012). Improving driving safety through automation. *National Highway Traffic Safety Administration*. https://www.nhtsa.gov/

He, X., Liu, Y., Lv, C., Ji, X., & Liu, Y. (2018). Emergency steering control of autonomous vehicle for collision avoidance and stabilization. *Vehicle System Dynamics, 57*(8), 1163–1187.

He, X., Liu, Y., Lv, C., Ji, X., & Liu, Y. (2019). Emergency steering control of autonomous vehicle for collision avoidance and stabilisation. *Vehicle system dynamics*, *57*(8), 1163-1187. https://doi.org/10.1080/00423114.2018.1537494

Zhao, Y. et al. (2021). A vehicle handling inverse dynamics method for emergency avoidance path tracking based on adaptive inverse control. *IEEE Transactions on Vehicular Technology, 70*(6), 5470–5482.

Zhao, Y., Pi, W., Zhang, W., Wang, Q., Feng, S., Deng, H., & Lin, F. (2021). A vehicle handling inverse dynamics method for emergency avoidance path tracking based on adaptive inverse control. *IEEE Transactions on Vehicular Technology*, *70*(6), 5470-5482. https://doi.org/10.1109/TVT.2021.3076870

Widrow, B., & Walach, E. (2008). Adaptive Inverse Control: A Signal Processing Approach. Piscataway.

Widrow, B., & Walach, E. (Eds.). (2008). *Adative Inverse Control: A Signal Processing Appr oach*. Wiley-IEEE Press. https://www.wiley.com/en-us/Adaptive+Inverse+Control%3A+A+Signal+Processing+Approach%2C+Reissue+Edition-p-9780470231609

P. Falcone, H. E. Tseng, J. Asgari, F. Borrelli, and D. Hrovat, "Integrated Braking And Steering Model Predictive Control Approach In Autonomous Vehicles," IFAC Proceedings Volumes, vol. 40, no. 10, pp. 273–278, 2007, doi: https://doi.org/10.3182/20070820-3-us-2918.00038.

Falcone, P., Tseng, H. E., Asgari, J., Borrelli, F., & Hrovat, D. (2007). Integrated braking and steering model predictive control approach in autonomous vehicles. *IFAC Proceedings Volumes*, *40*(10), 273-278.

https://doi.org/10.3182/20070820-3-us-2918.00038.

D. Pomerleau, "ALVINN: An Autonomous Land Vehicle in a Neural Network," vol. 1, no. -77, pp. 305–313, Jan. 1988, doi: https://doi.org/10.1184/r1/6603146.v1.

Pomerleau, D. A. (1988). Alvinn: An autonomous land vehicle in a neural network. *Advances in neural information processing systems*, *1*. : https://doi.org/10.1184/r1/6603146.v1

T. Shim, G. Adireddy, and H. Yuan, "Autonomous vehicle collision avoidance system using path planning and model-predictive-control-based active front steering and wheel torque control," Proceedings of the Institution of Mechanical Engineers, Part D: Journal of Automobile Engineering, vol. 226, no. 6, pp. 767–778, Jan. 2012.

Shim, T., Adireddy, G., & Yuan, H. (2012). Autonomous vehicle collision avoidance system using path planning and model-predictive-control-based active front steering and wheel torque control. *Proceedings of the Institution of Mechanical Engineers, Part D: Journal of automobile engineering*, *226*(6), 767-778. https://doi.org/10.1177/0954407011430275

S. Salehpour, Y. Pourasad, and S. H. Taheri, "Vehicle path tracking by integrated chassis control," Journal of Central South University, vol. 22, no. 4, pp. 1378–1388, Apr. 2015.

Salehpour, S., Pourasad, Y., & Taheri, S. H. (2015). Vehicle path tracking by integrated chassis control. *Journal of central south university*, *22*(4), 1378-1388. https://doi.org/10.1007/s11771-015-2655-y

W. Kim, D. Kim, K. Yi, and H. J. Kim, "Development of a path-tracking control system based on model predictive control using infrastructure sensors," Vehicle System Dynamics, vol. 50, no. 6, pp. 1001–1023, Jun. 2012.

Kim, W., Kim, D., Yi, K., & Kim, H. J. (2012). Development of a path-tracking control system based on model predictive control using infrastructure sensors. *Vehicle system dynamics*, *50*(6), 1001-1023. https://doi.org/10.1080/00423114.2011.597864

Hassanzadeh M, Lidberg M, and Keshavarz M. Path and speed control of a heavy vehicle for collision avoidance maneuvers. In: Intelligent vehicles symposium (IV), Alcala de Henares, Spain, 3–7 June 2012. pp. 129–134. IEEE.

Hassanzadeh, M., Lidberg, M., Keshavarz, M., & Bjelkeflo, L. (2012, June). Path and speed control of a heavy vehicle for collision avoidance manoeuvres. In *2012 IEEE intelligent vehicles symposium* (pp. 129-134). IEEE. https://doi.org/10.1109/IVS.2012.6232254

H. T. Cao, X. L. Song, S. Zhao, S. Bao, and Z. Huang, "An optimal model-based trajectory following architecture synthesizing the lateral adaptive preview strategy and longitudinal velocity planning for highly automated vehicle," Veh. Syst. Dyn., vol. 55, no. 8, pp. 1143-1188, Mar. 2017.

Cao, H., Song, X., Zhao, S., Bao, S., & Huang, Z. (2017). An optimal model-based trajectory following architecture synthesising the lateral adaptive preview strategy and longitudinal velocity planning for highly automated vehicle. *Vehicle system dynamics*, *55*(8), 1143-1188. https://doi.org/10.1080/00423114.2017.1305114

X. Zong, G. Xu, G. Yu, H. Su, and C. Hu, "Obstacle Avoidance for Self-Driving Vehicle with Reinforcement Learning," SAE International Journal of Passenger Cars - Electronic and Electrical Systems, vol. 11, no. 1, pp. 30–39, Sep. 2017.

Zong, X., Xu, G., Yu, G., Su, H., & Hu, C. (2017). Obstacle avoidance for self-driving vehicle with reinforcement learning. *SAE International Journal of Passenger Cars-Electronic and Electrical Systems*, *11*(07-11-01-0003), 30-39. https://doi.org/10.4271/07-11-01-0003

J. Ji, A. Khajepour, W. W. Melek, and Y. J. Huang, "Path planning and tracking for vehicle collision avoidance based on model predictive control with multiconstraints," IEEE Trans. Veh. Technol., vol. 66, no.2, pp. 952-964, Feb. 2017.

Ji, J., Khajepour, A., Melek, W. W., & Huang, Y. (2016). Path planning and tracking for vehicle collision avoidance based on model predictive control with multiconstraints. *IEEE transactions on vehicular technology*, *66*(2), 952-964 https://doi.org/10.1109/TVT.2016.2555853

C. Wnag, W. Zhao, Z. Xu, and G. Zhou, "Path planning and stability control of collision avoidance system based on active front steering," Science China Technological Sciences, vol. 60, no. 8, pp. 1231–1243, Apr. 2017.

Wnag, C., Zhao, W., Xu, Z., & Zhou, G. (2017). Path planning and stability control of collision avoidance system based on active front steering. *Science China Technological Sciences*, *60*(8), 1231-1243. https://doi.org/10.1007/s11431-016-9016-1

J. Guo, P. Hu, and R. Wang, "Nonlinear Coordinated Steering and Braking Control of Vision-Based Autonomous Vehicles in Emergency Obstacle Avoidance," IEEE Transactions on Intelligent Transportation Systems, vol. 17, no. 11, pp. 3230–3240, Nov. 2016.

Guo, J., Hu, P., & Wang, R. (2016). Nonlinear coordinated steering and braking control of vision-based autonomous vehicles in emergency obstacle avoidance. *IEEE Transactions on Intelligent Transportation Systems*, *17*(11), 3230-3240. https://doi.org/10.1109/TITS.2016.2544791

J. Shah, M. C. Best, A. Benmimoun, and Mohsen Lakehal Ayat, "Autonomous rear-end collision avoidance using an electric power steering system," vol. 229, no. 12, pp. 1638–1655, Feb. 2015.

Shah, J., Best, M., Benmimoun, A., & Ayat, M. L. (2015). Autonomous rear-end collision avoidance using an electric power steering system. *Proceedings of the Institution of Mechanical Engineers, Part D: Journal of Automobile Engineering*, *229*(12), 1638-1655. https://doi.org/10.1177/0954407014567517

Z. H. Peng, J. Wang, and Q. L. Han, "Path-Following Control of Autonomous Underwater Vehicles Subject to Velocity and Input Constraints via Neurodynamic Optimization," IEEE Trans. Ind. Electron., vol. 66, no. 11, pp. 8724-8732, Nov. 2019.

Peng, Z., Wang, J., & Han, Q. L. (2018). Path-following control of autonomous underwater vehicles subject to velocity and input constraints via neurodynamic optimization. *IEEE Transactions on Industrial Electronics*, *66*(11), 8724-8732. https://doi.org/10.1109/TIE.2018.2885726

D. Dong, H. Ye, W. Luo, J. Wen, and D. Huang, "Collision Avoidance Path Planning and Tracking Control for Autonomous Vehicles Based on Model Predictive Control," Sensors, vol. 24, no. 16, pp. 5211–5211, Aug. 2024, doi: https://doi.org/10.3390/s24165211.

Dong, D., Ye, H., Luo, W., Wen, J., & Huang, D. (2024). Collision avoidance path planning and tracking control for autonomous vehicles based on model predictive control. *Sensors*, *24*(16), 5211. https://doi.org/10.3390/s24165211

R. R. Wang et al., "Robust H_∞ path following control for autonomous ground vehicles with delay and data dropout," IEEE Trans. Intell. Transp. Syst., vol. 17, no. 7, pp. 2042-2050, Jul. 2016.

Wang, R., Jing, H., Hu, C., Yan, F., & Chen, N. (2016). Robust H_∞ path following control for autonomous ground vehicles with delay and data dropout. *IEEE Transactions on Intelligent Transportation Systems*, *17*(7), 2042-2050. https://doi.org/10.1109/TITS.2015.2498157

M. Chen, Y. Ren, and M. Ou, “Adaptive Robust Path Tracking Control for Autonomous Vehicles Considering Multi-Dimensional System Uncertainty,” World Electric Vehicle Journal, vol. 14, no. 1, p. 11, Jan. 2023.

Chen, M., Ren, Y., & Ou, M. (2023). Adaptive robust path tracking control for autonomous vehicles considering multi-dimensional system uncertainty. *World Electric Vehicle Journal*, *14*(1), 11. https://doi.org/10.3390/wevj14010011

R. Liu, M. Wei, and N. Sang, “Emergency obstacle avoidance trajectory tracking control based on active disturbance rejection for autonomous vehicles,” International Journal of Advanced Robotic Systems, vol. 17, no. 3, p. 172988142092110, May 2020.

Liu, R., Wei, M., & Sang, N. (2020). Emergency obstacle avoidance trajectory tracking control based on active disturbance rejection for autonomous vehicles. *International Journal of Advanced Robotic Systems*, *17*(3), 1729881420921105. https://doi.org/10.1177/1729881420921105

E. Quintero-Manriquez, E. N. Sanchez, R. G. Harley, S. F. Li, and R. A. Felix, “Neural Inverse Optimal Control Implementation for Induction Motors via Rapid Control Prototyping,” IEEE Trans. On Power Electron., vol. 34, no. 6, pp. 5981-5992, Jun. 2019.

Quintero-Manriquez, E., Sanchez, E. N., Harley, R. G., Li, S., & Felix, R. A. (2018). Neural inverse optimal control implementation for induction motors via rapid control prototyping. *IEEE Transactions on Power Electronics*, *34*(6), 5981-5992. https://doi.org/10.1109/TPEL.2018.2870159

C. Hu, R. R. Wang, F. J. Yan, and N. Chen, “Output constraint control on path following of four-wheel independently actuated autonomous ground vehicles,” IEEE Trans. Veh. Technol., vol. 65, no. 6, pp. 4033-4043, Jun. 2016.

Hu, C., Wang, R., Yan, F., & Chen, N. (2015). Output constraint control on path following of four-wheel independently actuated autonomous ground vehicles. *IEEE Transactions on Vehicular Technology*, *65*(6), 4033-4043. https://doi.org/10.1109/TVT.2015.2472975

E. Bakker, L. Nyborg, and H. B. Pacejka, “Tyre modelling for use in vehicle dynamics studies,” SAE Trans., vol. 96, pp. 190-204, Feb. 1987.

Bakker, E., Nyborg, L., & Pacejka, H. B. (1987). *Tyre modelling for use in vehicle dynamics studies* (No. 870421). SAE technical paper. https://nuhuo08.github.io/control/pacejka87.pdf.